THE JOURNAL OF BIOLOGICAL CHEMISTRY VOL. 285, NO. 43, pp. 33394–33403, October 22, 2010

Identification of the Matriptase Second CUB Domain as the Secondary Site for Interaction with Hepatocyte Growth Factor Activator Inhibitor Type-1*[S]

Received for publication, February 18, 2010, and in revised form, July 2, 2010 Published, JBC Papers in Press, August 3, 2010, DOI 10.1074/jbc.M110.115816

Kuniyo Inouye[‡1], **Satoshi Tsuzuki**[§], **Makoto Yasumoto**[‡], **Kenji Kojima**[‡], **Seiya Mochida**[§], **and Tohru Fushiki**[§]

From the Laboratory of [‡]*Enzyme Chemistry and* [§]*Nutrition Chemistry, Division of Food Science and Biotechnology, Graduate School of Agriculture, Kyoto University, Sakyo-ku, Kyoto City 606-8502, Japan*

Matriptase is a type II transmembrane serine protease comprising 855 amino acid residues. The extracellular region of matriptase comprises a noncatalytic stem domain (containing two tandem repeats of complement proteases C1r/C1s-urchin embryonic growth factor-bone morphogenetic protein (CUB) domain) and a catalytic serine protease domain. The stem domain of matriptase contains site(s) for facilitating the interaction of this protease with the endogenous inhibitor, hepatocyte growth factor activator inhibitor type-1 (HAI-1). The present study aimed to identify these site(s). Analyses using a secreted variant of recombinant matriptase comprising the entire extracellular domain (MAT), its truncated variants, and a recombinant HAI-1 variant with an entire extracellular domain (HAI-1–58K) revealed that the second CUB domain (CUB domain II, Cys^{340}–Pro^{452}) likely contains the site(s) of interest. We also found that MAT undergoes cleavage between Lys^{379} and Val^{380} within CUB domain II and that the C-terminal residues after Val^{380} are responsible for facilitating the interaction with HAI-1–58K. A synthetic peptide corresponding to Val^{380}–Asp^{390} markedly increased the matriptase-inhibiting activity of HAI-1–58K, whereas the peptides corresponding to Val^{380}–Val^{389} and Phe^{382}–Asp^{390} had no effect. HAI-1–58K precipitated with immobilized streptavidin resins to which a synthetic peptide Val^{380}–Pro^{392} with a biotinylated lysine residue at its C terminus was bound, suggesting direct interaction between CUB domain II and HAI-1. These results led to the identification of the matriptase CUB domain II, which facilitates the primary inhibitory interaction between this protease and HAI-1.

Matriptase (also known as epithin, membrane-type serine protease 1, SNC19, suppression of tumorigenicity 14) is a transmembrane serine protease (1–7). This protease belongs to the type II transmembrane serine protease group, which is characterized by an N-terminal cytoplasmic domain, a signal anchor transmembrane domain, and an extracellular C-terminal serine protease catalytic domain (8, 9). Matriptase is first synthesized as a zymogen comprising 855 amino acid residues in the human, mouse, and rat (7, 10, 11). Interaction between the zymogens appears to result in the generation of disulfide-linked two-chain molecules with an N-terminal Val^{615} (activated matriptase molecules) (Fig. 1*A*) (10, 12–16). In addition, matriptase appears to function both as a plasma membrane-associated form and as a shed (soluble) form (1, 15, 17). The two-chain matriptase purified from human milk exhibits activity with trypsin-like specificity and is known to cleave and thus activate single-chain urokinase-type plasminogen activator (sc-uPA)[2] and pro-hepatocyte growth factor (pro-HGF) (18). Bacterially expressed variants of the recombinant (r-) catalytic domain of matriptase also cleaved to activate sc-uPA (19) and pro-HGF (20). Another r-matriptase catalytic domain cleaved to activate the precursor form of prostasin, a glycosylphosphatidylinositol-linked serine protease (3, 21). Together with the abundant expression in epithelial cells and in keratinocytes (7, 22, 23), these characteristics lead to the proposition that matriptase plays a key role in the maintenance of epithelial integrity and homeostasis. Studies in genetically manipulated mice indicate the importance of matriptase for epithelial and epidermal barrier function (24–27).

In general, members of the type II transmembrane serine protease group have an extracellular noncatalytic stem domain comprising various structural motifs (8, 9). For instance, the stem domain of matriptase comprises a sea-urchin sperm protein-enteropeptidase-agrin (SEA) domain, followed by two tandem repeats of complement proteases C1r/C1s-urchin embryonic growth factor-bone morphogenetic protein (CUB) domain and four tandem repeats of a low-density lipoprotein receptor class A (LDLRA) domain (Fig. 1*A*) (7, 10, 11). In most members, however, the roles of the stem domain in their biological activities remain to be determined. To investigate the role of the matriptase stem domain, we prepared secreted variants of rat r-matriptase comprising the entire extracellular domain (pro-MAT, Tyr^{81}–Val^{855}) or only the catalytic domain (pro-CDMAT, Cys^{604}–Val^{855}) in a Chinese hamster ovary (CHO) cell-based expression system (Fig. 1*A*) (28, 29). The r-matriptase variants were purified in the pseudozymogen form

* This study was supported in part by Grants-in-aid for Scientific Research (Nos. 17380065 and 20380061, to K. I.) from the Japan Society for the Promotion of Science.

[S] The on-line version of this article (available at http://www.jbc.org) contains supplemental Fig. S1.

[1] To whom correspondence should be addressed. Tel.: 81-75-753-6266; Fax: 81-75-753-6265; E-mail: inouye@kais.kyoto-u.ac.jp.

[2] The abbreviations used are: sc-uPA, single-chain urokinase-type plasminogen activator; Boc, *t*-butyloxycarbonyl; CHO, Chinese hamster ovary; CUB domain, complement proteases C1r/C1s-urchin embryonic growth factor-bone morphogenetic protein domain; HAI-1, hepatocyte growth factor activator inhibitor type-1; HGF, hepatocyte growth factor; LDLRA domain, low-density lipoprotein receptor class A domain; MCA, 4-methyl-coumaryl-7-amide; r-EK, recombinant form of enteropeptidase; SEA domain, sea-urchin sperm protein-enteropeptidase-agrin domain.

and then converted to the two-chain active form by incubation with a recombinant form of enteropeptidase (also known as enterokinase) (hereinafter r-EK) *in vitro* (Fig. 1*A*) (28, 29). The activities toward various peptidyl-4-methyl-coumaryl-7-amide (MCA) substrates containing an Arg residue at the P1 site and sc-uPA did not substantially differ between the r-matriptase variants treated with r-EK (29). This suggested that the matriptase stem domain has no substantial effect on its own catalytic activity.

HGF activator inhibitor type-1 (HAI-1) is a Kunitz-type serine protease inhibitor (30). HAI-1 is thought to be responsible for regulating matriptase activity *in vivo* (1, 13, 26, 28, 31). This inhibitor is produced first as a type I transmembrane protein with a molecular mass of 66 kDa (refer to Fig. 1*B*), and the extracellular domain is then shed (30, 32). HAI-1 species with molecular masses of 58 kDa and 40 kDa appear in culture media conditioned by human gastric carcinoma MKN45 cells (30, 32) or by monkey kidney COS-1 cells transfected with a cDNA encoding the full-length rat HAI-1 (33, 34). The 58-kDa species has the entire extracellular domain, which comprises an N-terminal domain, followed by an internal domain, the first protease inhibitory domain (Kunitz domain I), an LDLRA domain, and the second Kunitz domain (Kunitz domain II). The 40-kDa species is thought to lack the LDLRA domain and Kunitz domain II (30, 32). Using secreted variants of rat r-HAI-1, we found that Kunitz domain I exhibits inhibitory activity against r-EK-treated pro-MAT but the Kunitz domain II does not (28). Rather, the Kunitz domain II interrupts the matriptase-inhibiting activity of Kunitz domain I. A variant of r-HAI-1 corresponding to the 58-kDa species (designated HAI-1–58K, refer to Fig. 1*B*) inhibited r-EK-treated pro-MAT with considerably less efficiency than did the variant corresponding to the 40-kDa species (designated HAI-1–40K, refer to Fig. 1*B*) (28).

We also found that r-EK-treated pro-MAT is more strongly inhibited by HAI-1–58K than is r-EK-treated pro-CDMAT in the hydrolysis of *t*-butyloxycarbonyl (Boc)-[(2*S*)-2-amino-3-(benzyloxycarbonyl-propionyl)-L-prolyl-L-arginine-MCA [Boc-D(OBzl)PR-MCA] (35). This suggests that the matriptase stem domain contains site(s) that facilitate the inhibitory interaction between the protease and inhibitor. In the present study, we identified the second CUB domain (CUB domain II, Cys^{340}–Pro^{452}) as the site of interest.

EXPERIMENTAL PROCEDURES

Materials—Bovine r-EK (Recombinant Enterokinase®), immobilized S-protein (S-protein®-agarose), S-protein conjugated with horseradish peroxidase, and pT7blue2 vector were purchased from Novagen (Madison, WI). Boc-D(OBzl)PR-MCA and Boc-L-glutamyl-L-alanyl-L-arginine-MCA (Boc-QAR-MCA) were purchased from Peptide Institute (Osaka, Japan). Spectrozyme tPA® (Sp-tPA, methylsulfonyl-D-cyclohexyltyrosyl-glycyl-L-arginine-*p*-nitroanilide acetate) was purchased from American Diagnostica (Greenwich, CT). Bovine trypsinogen and trypsin (type III) were purchased from Sigma. Restriction endonucleases and a protein size marker (Prestained Protein Marker, broad range) were purchased from New England Biolabs (Beverly, MA). KOD_{-plus-}DNA polymerase, T4 polynucleotide kinase, and a DNA ligation kit were purchased from Toyobo (Osaka, Japan). Reagents for cell culture and synthetic oligonucleotides were purchased from Invitrogen (Carlsbad, CA). Eight peptides (C2 peptides: C2P1, C2P2, C2P3, C2P4, C2P5, C2P6, C2P7, and C2P8) were synthesized by and purchased from Biosynthesis, Inc. (Lewisville, TX). A 12-amino acid-C2 peptide with a biotinylated lysine residue at the C terminus (C2P9-biotin) was synthesized by and purchased from GenixTalk (Osaka, Japan). An immobilized streptavidin (ImmunoPure® Immobilized Streptavidin Gel) was purchased from Pierce. All other reagents were of analytical grade and were purchased from Nacalai Tesque (Kyoto, Japan).

Construction of Expression Plasmids—Plasmids for the expression of pro-MAT (pSec-ekMT-SP1s), pro-CDMAT (pSec-L-matriptase), HAI-1–58K (pSec-HAI-1–58K), HAI-1–40K (pSec-HAI-1–40K), and HAI-KD2 (pSec-HAI-KD2) were constructed using pSecTag2/HygroB vector (Invitrogen) (28, 29, 35, 36).

The plasmid for expression of pro-ΔS-MAT (Gln^{210}–Val^{855}) was created as follows: A DNA fragment was amplified by polymerase chain reaction (PCR) with KOD_{-plus-}DNA polymerase, 5′-TCAGGACAACAGCTGCA-3′ and 5′-CTATACCCCAGTTTGCTCT-3′ as the forward and reverse primers, respectively, and pSec-ekMT-SP1s as the template. The PCR product was phosphorylated with T4 polynucleotide kinase and ligated into the SmaI-linearized pT7blue2 vector (pT7-ΔS-MAT). pT7-ΔS-MAT was digested with KpnI and BamHI, and the resulting fragment was ligated into pSec-L-matriptase from which a fragment produced by digestion with KpnI and BamHI had been removed (pSec-ΔS-MAT). Expression plasmids for pro-ΔSC1-MAT (Lys^{336}–Val^{855}) and pro-ΔSC1C2-MAT (Cys^{453}–Val^{855}) were made using the same method except that 5′-TAAGATGAGCAGCTGTGG-3′ and 5′-ATGCCCAGGGATGTTCAT-3′, respectively, were used as forward primers. The plasmids were designated pSec-ΔSC1-MAT and pSec-ΔSC1C2-MAT. The plasmid for expression of pro-S805A-MAT was created as follows: pcDNA-S805A-matriptase (14) was digested with BfuAI, and the resulting fragment was ligated into pSec-ekMT-SP1s from which a fragment produced by digestion with the same restriction endonuclease had been removed (pSec-S805A-MAT). The sequences of all the plasmids constructed in the present study were determined in both directions by the dideoxynucleotide chain-termination method as described previously (7).

Expression, Purification, and Treatment with r-EK of Pro-ΔS-, Pro-ΔSC1-, Pro-ΔSC1C2, and Pro-S805A-MAT Variants—A CHO-K1 cell line was maintained in Ham's F12 medium containing 5% fetal bovine serum. pSec-ΔS-MAT, pSec-ΔSC1-MAT, pSec-ΔSC1C2-MAT, and pSec-S805A-MAT were transfected into the cell line as described previously (28). Cells resistant to Ham's F12 medium containing 200 μg/ml hygromycin B (Invitrogen) were propagated and stored in liquid nitrogen until use.

Samples of the frozen cells were thawed and cultured in 75-cm^2 flasks (Asahi Techno Glass, Tokyo) until confluent. Cells were washed three times with phosphate-buffered saline (8 mM Na_2HPO_4, 1.5 mM KH_2PO_4, 136 mM NaCl, and 2.7 mM KCl, pH 7.4), and 10 ml of serum-free Ham's F12 was added to each flask. After 48 h, the conditioned medium was collected,

and fresh serum-free medium was added. This was repeated until half of the cells had peeled off. The collected media were centrifuged immediately at 3,000 × *g* for 10 min at 4 °C, and the resulting supernatants were stored at −20 °C until use.

For purification, 200 ml of the conditioned medium were collected into two flasks. After thawing, the medium conditioned by CHO-K1 cells transfected with pSec-ΔS-MAT, pSec-ΔSC1-MAT, pSec-ΔSC1C2-MAT, and pSec-S805A-MAT were pooled and concentrated to 2.5 ml by ultrafiltration using Amicon® Ultra-15 filter unit (30,000 MWCO; Millipore, Tokyo, Japan) and Amicon® Ultra-15 (50,000 MWCO), respectively. The concentrated medium was subjected to gel filtration in 25 mM HEPES-NaOH (pH 7.5) buffer containing 145 mM NaCl and 0.1% Triton X-100 (HEPES buffer) using a PD-10 column (GE Healthcare, Tokyo, Japan) with an elution volume of 3.5 ml. A 0.5-ml sample of the gel filtrates was incubated for 30 min with 25 μl of a slurry of immobilized S-protein at 22 °C with rocking. After centrifugation at 5,000 × *g* for 2 s at 22 °C, the resulting supernatant was incubated again with fresh immobilized S-protein as described above. After centrifugation at 5,000 × *g* for 2 s at 22 °C, the resulting supernatant was discarded. Slurries were pooled (total 175 μl for each variant) and washed extensively with HEPES buffer. The r-matriptase variants bound to the slurry were eluted by incubating with rocking for 10 min at 22 °C with 500 μl of HEPES buffer containing 10 μM 15-amino acid S-tag peptide (KETAAAKFERQHIDS, synthesized by and purchased from BEX, Tokyo, Japan). To collect the eluate, each mixture was transferred to a spin column (Attoprep™, Atto, Tokyo, Japan) and centrifuged at 5,000 × *g* for 1 min at 22 °C. The eluates were subjected to gel filtration in HEPES buffer using an NAP-5 column (GE Healthcare) with an elution volume of 1.0 ml and stored at −20 °C until use.

A 0.5-μl sample of r-EK (2 units/μl) was added to 500 μl of HEPES buffer containing one of the r-matriptase variants, and the mixture (activation mixture) was incubated for 24 h at 22 °C. After incubation, the activation mixture was stored at −20 °C until use.

Preparation of pro-MAT, pro-CDMAT, HAI-1–58, HAI-1–40K, and HAI-KD2—pro-MAT, pro-CDMAT, HAI-1–58K, HAI-1–40K, and HAI-KD2 have been expressed in and secreted by CHO-K1 cells (28, 29, 35). pro-MAT and pro-CDMAT variants were purified and treated with r-EK as described above except that Amicon® Ultra-15 (50,000 MWCO) and Amicon® Ultra-15 (10,000 MWCO) filter units were used for medium condensation, respectively. Methods for purification and determination of the concentration of HAI-1–58K, HAI-1–40K, and HAI-KD2 were described in detail previously (28).

Treatment of r-EK-treated pro-MAT with Immobilized Benzamidine—A 0.5-ml sample of HEPES buffer containing r-EK-treated pro-MAT was incubated for 30 min with 50 μl of a slurry of immobilized benzamidine (benzamidine-Sepharose 6B; GE Healthcare) at 22 °C with rocking. After centrifugation at 5,000 × *g* for 2 s at 22 °C, the resulting supernatant was incubated again with fresh immobilized benzamidine as described above. After centrifugation at 5,000 × *g* for 2 s at 22 °C, the resulting supernatant was collected and stored at −20 °C until use. Slurries were pooled (100 μl) and washed extensively with HEPES buffer. The r-matriptase variants bound to the slurry were then eluted by incubating with rocking for 10 min at 22 °C with 500 μl of 25 mM HEPES-NaOH (pH 7.5) buffer containing 1 M NaCl and 0.1% Triton X-100. The mixture was transferred to an Attoprep and centrifuged at 5,000 × *g* for 1 min at 22 °C. The eluate was subjected to gel filtration in HEPES buffer using an NAP-5 column and stored at −20 °C until use.

Sodium Dodecyl Sulfate-Polyacrylamide Gel Electrophoresis and Western blot Analysis—A 24-μl part of the samples was mixed with 6 μl of 5× Laemmli protein sample buffer (Laemmli buffer) (1× Laemmli buffer: 0.05 M Tris-HCl (pH 6.8), 10% glycerol, 2% SDS, 0.005% bromphenol blue) (37). The samples were boiled for 3 min in the presence or absence of 12 mM dithiothreitol, cooled, and subjected to SDS-PAGE. After separation, the proteins were transferred by electroblotting onto a polyvinylidene difluoride (PVDF) membrane (Fluorotrans W; Nihon Genetics, Tokyo, Japan). After washing with 50 mM Tris-HCl, pH 7.5, buffer containing 150 mM NaCl and 0.1% Tween 20 (TBST), the blots were incubated with a rabbit anti-rat matriptase catalytic domain antibody (Spr992, a polyclonal antibody raised against rat matriptase residues Ser^{686} to Arg^{696}) diluted in an immunoreaction-enhancer solution (Can Get Signal® Solution I; Toyobo) (1:20 dilution) (34). After washing with TBST, the blots were incubated with a horseradish peroxidase-conjugated goat anti-rabbit IgG antibody (Dako Japan, Kyoto) diluted in another immunoreaction-enhancer solution (Can Get Signal® Solution II; Toyobo) (1:3000 dilution). After washing the blots with TBST, the protein bands were visualized using an ECL® detection system (GE Healthcare). r-HAI-1 variants were probed with S-protein conjugated with horseradish peroxidase diluted in Can Get Signal® Solution II (1:3000 dilution).

N-terminal Sequencing—pro-MAT molecules before and after r-EK treatment were subjected to SDS-PAGE (12% polyacrylamide) under either reducing or nonreducing conditions. Following SDS-PAGE, the proteins were transferred onto a PVDF membrane and stained with Coomassie Brilliant Blue. The portion of the membrane where the protein bands of interest were detected was excised and subjected to N-terminal sequencing with an automated protein sequencer (Procise 494 cLC; Applied Biosystems, Tokyo, Japan) (38, 39).

Determination of Concentrations of the r-Matriptase Variants Treated with r-EK—Sp-tPA was dissolved in distilled water at a concentration of 5 mM and stored at −20 °C until use. A 2-μl part of the activation mixture (see above) was added to 38 μl of HEPES buffer containing 250 μM Sp-tPA, and the mixture was incubated for 10 min at 37 °C. The reaction was terminated by adding 400 μl of 0.1 M sodium acetate (pH 4.3) buffer containing 100 mM monochloroacetic acid, and the absorbance at 405 nm was measured. The initial rate of hydrolysis was determined using the molar absorption coefficient ϵ_{405} of 9.65 $mM^{-1}\ cm^{-1}$ for *p*-nitroaniline. One unit of activity was defined as the amount of the enzyme that liberates 1 nmol of *p*-nitroaniline from Sp-tPA, and the enzyme concentration was estimated by SDS-PAGE (12% polyacrylamide) under reducing conditions followed by silver staining with bovine trypsinogen as the standard. One enzyme unit of activity was produced by 80

fmol of enzyme. Under these assay conditions, r-EK (final concentration: 0.05 mU/μl) exhibited no detectable activity toward Sp-tPA.

Inhibition Assay—Boc-D(OBzl)PR-MCA was dissolved in dimethyl sulfoxide at a concentration of 20 mM and stored at −20 °C until use. Each r-matriptase variant treated with r-EK (activation mixture) was diluted with HEPES buffer at a concentration of 20 nM; the concentration of r-EK remained in the range of 0.05–0.4 mU/μl in the diluted activation mixture. The inhibition assay was conducted as follows. Various concentrations of HAI-1–58K and HAI-1–40K were preincubated for 5 min at 37 °C in 38 μl of HEPES buffer containing 1.1 mM Boc-D(OBzl)PR-MCA, and the hydrolysis of the substrate was initiated by adding 2 μl of diluted activation mixture. After further incubation for 2 h at 37 °C, the reaction was terminated as described above. The absorbance at 370 nm of the product 4-methyl-coumaryl-7-amine was measured. The initial reaction rate (v_o) of the hydrolysis was determined using the molar absorption coefficient of 7.7 mM^{-1} cm^{-1} of 4-methyl-coumaryl-7-amine. Under the assay conditions, r-EK (final concentration: 0.02 mU/μl) exhibited no detectable activity toward Boc-D(OBzl)PR-MCA.

Reaction between r-EK-treated r-Matriptase Variants and r-HAI-1 Variants in the Presence of C2 Peptides—C2 peptides (C2P1-C2P8) were dissolved in dimethyl sulfoxide at a concentration of 2 mM and stored at −20 °C until use. HAI-1–58K and HAI-1–40K were preincubated for 5 min at 37 °C in 38 μl of HEPES buffer containing 1.1 mM Boc-D(OBzl)PR-MCA and C2 peptides, and the hydrolysis of the substrate was initiated by adding 2 μl of HEPES buffer containing 40 nM of the r-matriptase variants and 0.05 mU/μl of r-EK. The reactions were performed, and the v_o values were determined as described above.

Binding of r-HAI-1 Variants to the Immobilized C2P9-Biotin—C2P9-biotin was dissolved in dimethyl sulfoxide at a concentration of 10 mM and stored at −20 °C until use. 100 nmol of C2P9-biotin dissolved in 500 μl of HEPES buffer was incubated with a 50-μl slurry of immobilized streptavidin in a microcentrifuge tube for 2 h at 22 °C with rocking. The resin was washed three times with HEPES buffer, and 1 pmol of HAI-1–58K, HAI-1–40K, or HAI-KD2 dissolved in 500 μl of the buffer was added. The mixture was incubated for 2 h at 22 °C with rocking. The proteins bound to resin were eluted by boiling in the presence of 1× Laemmli buffer and analyzed by SDS-PAGE and Western blotting with S-protein conjugated with horseradish peroxidase (28).

RESULTS

Characterization of r-Matriptase Variants—Pseudozymogen forms of r-matriptase (pro-MAT and pro-CDMAT) had been produced previously in CHO-K1 cells (Fig. 1*A*) (28, 29). In the present study, we prepared an additional three truncated variants of pro-MAT: pro-ΔS-MAT, in which the SEA domain was deleted; pro-ΔSC1-MAT, in which the SEA domain and the first CUB domain (CUB domain I) were deleted; and pro-ΔSC1C2-MAT, in which the SEA domain and both CUB domains were deleted (Fig. 1*A*). These truncated variants were also expressed in CHO-K1 cells. The expression vector used (pSecTag2-HygroB) contains the sequence of immunoglobulin κ signal peptide allowing for secretion of translation products from mammalian cells. All variants were fused to S-tag at their N termini. This fusion is convenient for purification by affinity chromatography using immobilized S-protein. Importantly, five amino acid residues needed for activation cleavage of this protease (Thr-Lys-Gln-Ala-Arg^{614}) were changed to those suitable for the cleavage by enteropeptidase (Asp-Asp-Asp-Asp-Lys) in any of variants. This allowed for activation of the variants (*i.e.* generation of an N-terminal valine residue corresponding to matriptase Val^{615}) by treatment with r-EK.

The culture medium conditioned by CHO-K1 cells stably transfected with pSec-ΔS-MAT, pSec-ΔSC1-MAT, or pSec-ΔSC1C2-MAT were concentrated, gel-filtered, and treated with an immobilized S-protein. The precipitants with S-protein resin, together with purified pro-MAT and pro-CDMAT variants, were separated by SDS-PAGE under reducing conditions. After Western transfer, the blot was probed with an anti-rat matriptase catalytic domain antibody named Spr992 (33, 34). Samples of pro-MAT and pro-CDMAT variants have been found to produce signals at the position corresponding to 90 kDa and 40/38/33/31 kDa, respectively (refer to Fig. 2, *lanes 1* and *5*) (28, 29). Appearance of the many bands of pro-CDMAT may be due to cleavage by signal peptidases of CHO-K1 cells at differential sites. In the present study, we determined the N-terminal sequence of the 90 kDa protein produced by pro-MAT to be SVIAY. This indicates that like full-length matriptase, pro-MAT is processed post-translationally via cleavage between Gly^{149} and Ser^{150} within the SEA domain and that the fragment Ser^{150}–Val^{855} is associated with the fragment containing matriptase Tyr^{81}–Gly^{149} (refer to Fig. 1*A*) (11, 33, 39). Samples of pro-ΔS-, pro-ΔSC1-, and pro-ΔSC1C2-MAT variants produced dense signals at the 90-, 75-, and 62-kDa positions, respectively (Fig. 2, *lanes 2–4*).

Purified pseudozymogen forms of r-matriptase were treated with r-EK and then analyzed by SDS-PAGE and Western blotting with Spr992. r-EK-treated pro-MAT and r-EK-treated pro-CDMAT have been found to produce a dense signal at the 30-kDa position (refer to Fig. 2, *lanes 6* and *10*) (28, 29). The N-terminal sequence of the 30-kDa band produced from a sample of r-EK-treated pro-MAT was determined to be VVGGT (refer to Fig. 1*A*). Comparable results were obtained from samples of pro-ΔS-, pro-ΔSC1-, and pro-ΔSC1C2-MAT variants treated with r-EK (Fig. 2. *lanes 7–9*). These results indicate that, like the pro-MAT and pro-CDMAT variants, pro-ΔS-, pro-ΔSC1-, and pro-ΔSC1C2-MAT variants are cleaved by r-EK at the N-terminal peptide bond of the residue corresponding to matriptase Val^{615} (refer to Fig. 1*A*).

The catalytic activity of matriptase has been evaluated quantitatively using the hydrolysis of a chromogenic substrate, Sp-tPA (10, 14, 28, 40). r-EK-treated pro-MAT and r-EK-treated pro-CDMAT exhibited similar activity toward the substrate (28, 40). The two r-EK-treated r-matriptase variants have also been found to cleave various peptidyl-MCA substrates with an arginine residue existing at the P1 site (29). Among the substrates tested, Boc-QAR-MCA and Boc-D(Obzl)PR-MCA are most preferred (28, 29). The initial rates of hydrolysis of Boc-QAR-MCA and Boc-D(Obzl)PR-MCA catalyzed by pro-ΔS-,

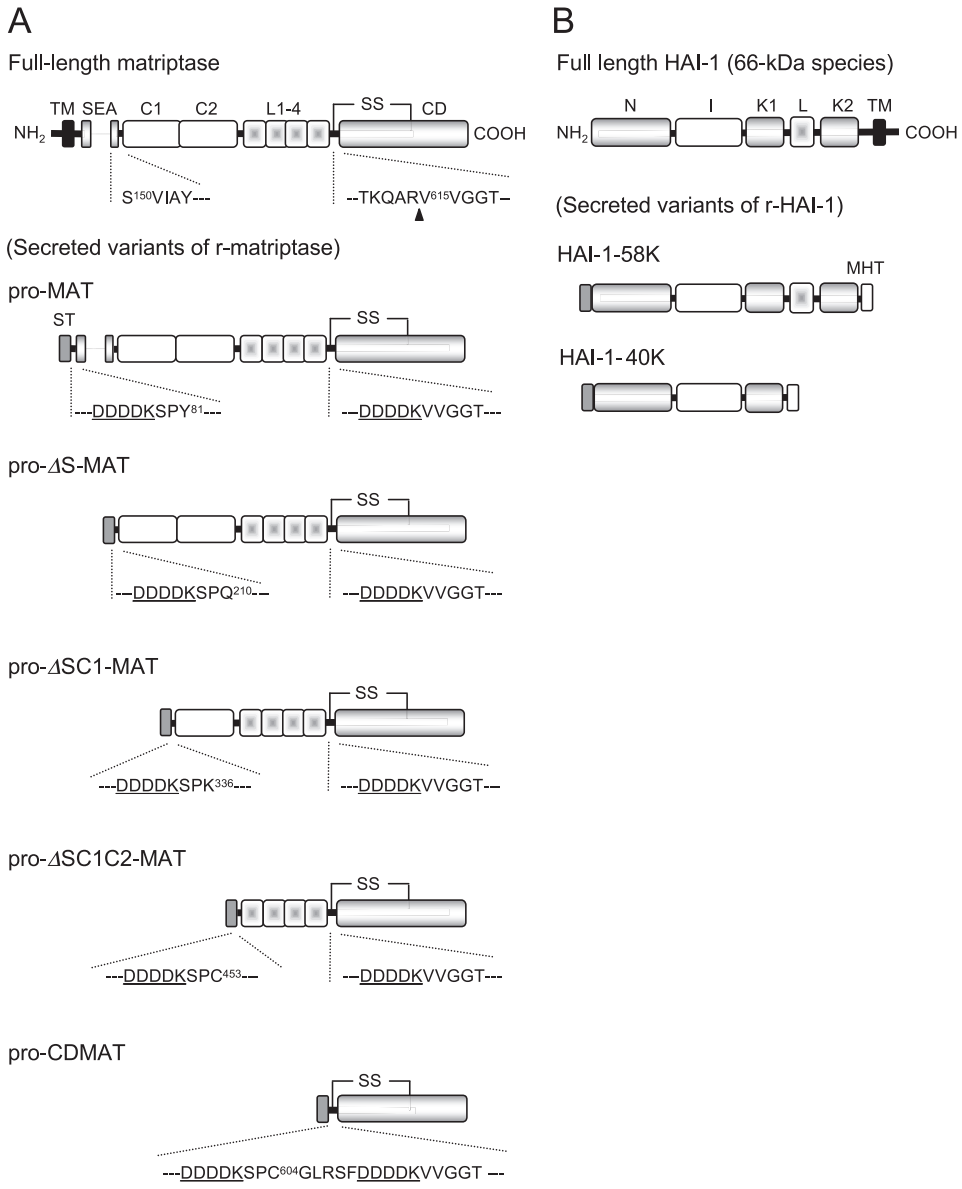

FIGURE 1. **Schematic illustration of the structure of rat matriptase and rat HAI-1 and their expression constructs.** *A*, domain structures of full-length rat matriptase (*top*) and r-matriptase variants. The amino acid numbering starts from the putative N terminus of the protein. The N and C termini are indicated by NH_2 and *COOH*, respectively, in the full-length matriptase. The amino acid sequence around the matriptase activation cleavage site is indicated in the single-letter code by amino acid numbering at the N-terminal Val residue of the catalytic domain (Val^{615}). The activation-cleavage site is indicated by the *arrowhead*. Matriptase is known to undergo post-translational processing via cleavage between Gly^{149} and Ser^{150} within the SEA domain (28). The five amino acid sequence starting from Ser^{150} is indicated. The association between Met^{1}–Gly^{149} and Ser^{150}–Val^{855} is indicated by the *dotted line*. pro-MAT is a secreted variant of r-matriptase in which the cytosolic domain and the signal anchor (Met^{1}–His^{80}) are replaced by the human immunoglobulin κ-chain signal peptide and S-tag (ST). Like full-length matriptase, pro-MAT undergoes processing via cleavage after the residue corresponding to matriptase Gly^{149}. pro-ΔS-MAT, pro-ΔSC1-MAT, and pro-ΔSC1C2-MAT are truncated variants of pro-MAT. pro-CDMAT is a variant comprising only the catalytic domain. Enteropeptidase recognition sequences (DDDDK, *underlined*) and their surrounding sequences are shown in all r-matriptase variants. Note that the S-tag at the N terminus of each variant can also be removed by incubation with r-EK. The amino acid sequence around the first enteropeptidase recognition site is indicated by amino acid numbering of the residues of each variant (Tyr^{81}, Gln^{210}, Lys^{336}, Cys^{453}, and Cys^{604}). The predicted disulfide linkages between two cysteine residues corresponding to Cys^{604} and Cys^{731} in the matriptase and r-matriptase molecules are shown as *SS*. *TM*, transmembrane domain; *SEA*, SEA domain; *C1* and *C2*, CUB domain I and CUB domain II, respectively; L1–4, four repeats of the LDLRA domain; *CD*, catalytic domain. *B*, domain structures of full-length HAI-1 (66-kDa species) and secreted variants of r-HAI-1 (HAI-1–58K and HAI-1–40K). The N and C termini are indicated by NH_2 and *COOH*, respectively, in the full-length HAI-1. HAI-1–58K and HAI-1–40K are secreted variants of r-HAI-1 corresponding to the 58-kDa and 40-kDa species, respectively. S-tag (*ST*) and Myc epitope-hexahistidine tag (*MHT*) are fused at their N and C termini, respectively. *N*, N-terminal domain; *I*, internal domain; *K1*, Kunitz domain I; *L*, LDLRA domain; *K2*, Kunitz domain II; *TM*, transmembrane domain.

pro-ΔSC1-, and pro-ΔSC1C2-MAT variants treated with r-EK were similar to those catalyzed by pro-MAT and pro-CDMAT variants treated with r-EK. Hereinafter, pro-MAT, pro-ΔS-MAT, pro-ΔSC1-MAT, pro-ΔSC1C2-MAT, and pro-CDMAT variants treated with r-EK are referred to as simply MAT, ΔS-MAT, ΔSC1-MAT, ΔSC1C2-MAT, and CDMAT variants, respectively.

Inhibition of r-Matriptase Variants by HAI-1–58K and HAI-1–40K—We produced secreted variants of r-HAI-1 (HAI-1–58K and HAI-1–40K) (refer to Fig. 1*B*). Using Boc-D(Obzl)PR-MCA as the substrate in a previous study, we found that MAT is inhibited more strongly by HAI-1–58K than is CDMAT but that the r-matriptase variants are inhibited by HAI-1–40K with similar efficiency (35).

In the present study, we examined the inhibition by HAI-1–58K or HAI-1–40K of ΔS-, ΔSC1-, and ΔSC1C2-MAT variants using Boc-D(Obzl)PR-MCA as the substrate. Note that r-EK exhibited weak activity toward Boc-QAR-MCA but did no detectable activity toward Boc-D(Obzl)PR-MCA and that r-EK was not inhibited by the r-HAI-1 variants in the hydrolysis of Boc-QAR-MCA. These findings indicate that r-EK does not seriously affect the inhibitory interaction of r-matriptase variants with r-HAI-1 variants in the hydrolysis of Boc-D(Obzl)PR-MCA.

ΔS- and ΔSC1-MAT variants were inhibited by HAI-1–58K similarly to MAT (Fig. 3, *upper panel*). ΔSC1C2-MAT was inhibited similarly to CDMAT (Fig. 3, *upper panel*). The concentrations of HAI-1–58K required for 50% inhibition (IC_{50}) of MAT, ΔS-MAT, ΔSC1-MAT, ΔSC1C2-MAT, and CDMAT variants were 11.5, 12.1, 11.7, >100, and >100 nM, respectively. These results suggest that the stronger inhibition of MAT than of CDMAT is attributed to the presence of CUB domain II. The five r-matriptase variants were inhibited by HAI-1–40K with similar

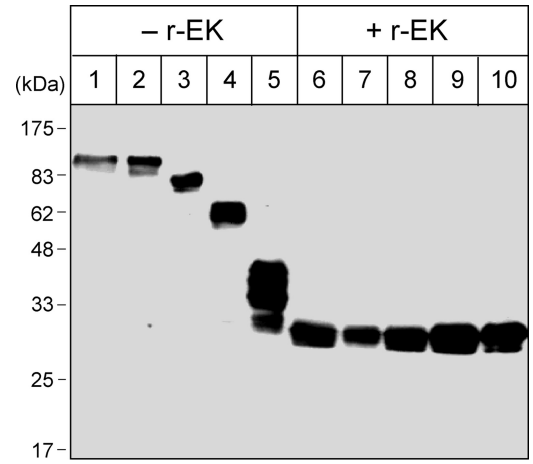

FIGURE 2. **Western blot analysis of r-matriptase variants.** Samples of r-matriptase variants before (−) and after (+) r-EK treatment were separated by SDS-PAGE (12% polyacrylamide) under reducing conditions. *Lanes 1* and *6*, pro-MAT; *lanes 2* and *7*, pro-ΔS-MAT; *lanes 3* and *8*, pro-ΔSC1-MAT; *lanes 4* and *9*, pro-ΔSC1C2-MAT; *lanes 5* and *10*, pro-CDMAT. After Western transfer, the blot was probed with Spr992. The molecular masses of the marker proteins are indicated on the *left* in kilodaltons (*kDa*).

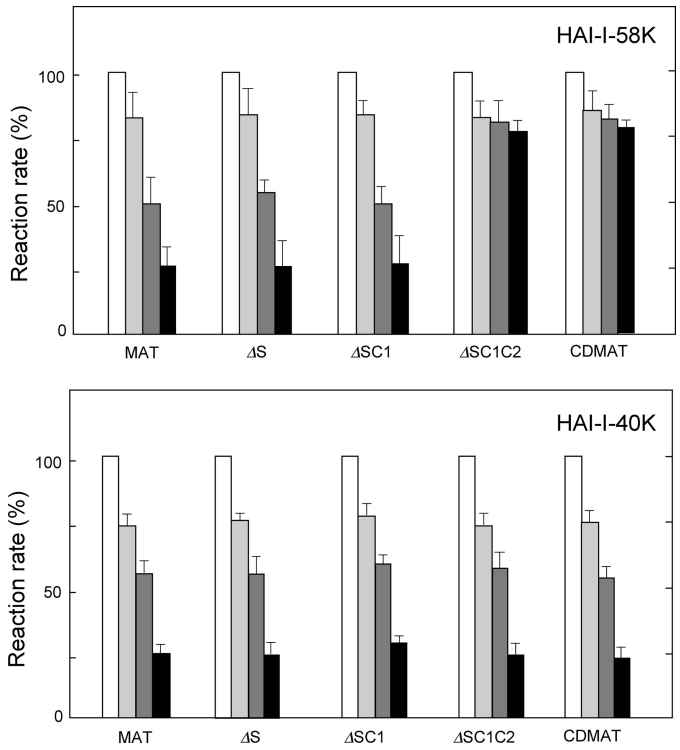

FIGURE 3. **Inhibition of r-matriptase variants by HAI-1–58K and HAI-1–40K.** The reactions were initiated by adding r-matriptase variants (MAT, Δ*S*-MAT (ΔS), ΔSC1-MAT (ΔSC1), ΔSC1C2-MAT (ΔSC1C2), and CDMAT variants) at a final concentration of 1 nM to the mixture containing inhibitor and substrate [Boc-D(Obzl)PR-MCA]. The concentrations of HAI-1–58K were 0 nM (*white*), 5 nM (*light gray*), 10 nM (*dark gray*), and 20 nM (*black*); the concentrations of HAI-1–40K were 0 nM (*white*), 0.5 nM (*light gray*), 1 nM (*dark gray*), and 2 nM (*black*). In each reaction mixture, the substrate was included at a final concentration of 1 mM. The initial rate of substrate hydrolysis in the absence of inhibitor was about 4 nM s^{-1} and was taken as 100% in each r-matriptase variant. All values are expressed as means ± S.D. of triplicate determination.

efficiency (Fig. 3, *lower panel*). The IC_{50} values for the inhibitory activity against all the r-matriptase variants were similar (around 1.2 nM). This indicates that CUB domain II does not affect the inhibitory interaction with HAI-1–40K.

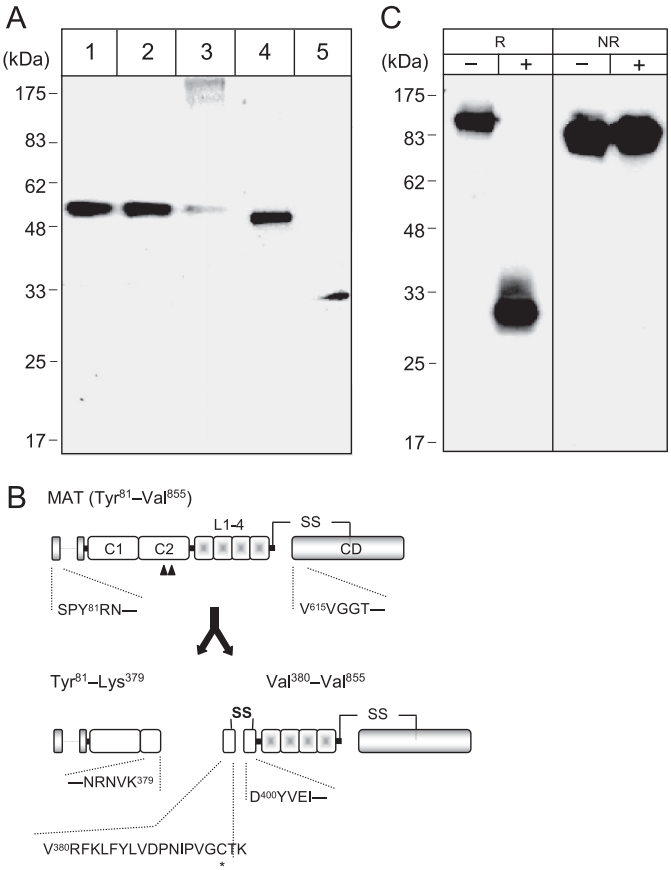

FIGURE 4. **Cleavage of MAT within its CUB domain II.** *A*, Western blot analysis. A sample of MAT, together with those of ΔS-MAT, ΔSC1-MAT, ΔSC1C2-MAT, and CDMAT, was separated by SDS-PAGE (12% polyacrylamide) under nonreducing conditions. *Lane 1*, MAT; *lane 2*, ΔS-MAT; *lane 3*, ΔSC1-MAT; *lane 4*, ΔSC1C2-MAT; *lane 5*, CDMAT. After Western transfer, the blot was probed with Spr992. The molecular masses of the marker proteins are indicated on the *left* in kilodaltons (*kDa*). *B*, schematic illustration of MAT molecules with and without cleavage at CUB domain II. MAT (before cleavage at CUB domain II) is shown on the *top*. The sites for cleavage in CUB domain II are indicated by the *arrowhead*. The N-terminal amino acid sequences of MAT and its catalytic domain are indicated in the single-letter code with amino acid numbering corresponding to matriptase Tyr^{81} and Val^{615}, respectively. Ser and Pro residues encoded by pT7blue2 vector are also indicated. Upon cleavage between Lys^{379} and Val^{380}, two fragments (Tyr^{81}–Lys^{379} and Val^{380}–Val^{855}) are generated. Although MAT also undergoes cleavage between Lys^{399} and Asp^{400}, fragment Val^{380}–Lys^{399} can be associated with fragment Asp^{400}–Val^{855} via an intramolecular disulfide bond formed between Cys^{397} and Cys^{410} (indicated by bold *SS*). The amino acid sequences of the C-terminal residues of fragment Tyr^{81}–Lys^{379}, of Val^{380}–Lys^{399}, and of N-terminal residues of Asp^{400}–Val^{855} are indicated in the single-letter code with amino acid numbering at Lys^{379}, Val^{380}, and Asp^{400}, respectively. Cys^{397} is indicated by the *asterisk*. The predicted disulfide linkages between Cys^{604} and Cys^{731} are shown as *SS*. The association between fragments $SerProTyr^{81}$–Gly^{149} and Gly^{149}–Lys^{379} is indicated by the *dotted line*. *C1* and *C2*, CUB domain I and CUB domain II, respectively; *L1–4*, four repeats of the LDLRA domain; *CD*, catalytic domain. *C*, Western blot analysis of active-site mutant of MAT. Samples of pro-S805A-MAT before (−) and after (+) r-EK treatment were separated by SDS-PAGE (12% polyacrylamide) under reducing (*R*) and nonreducing (*NR*) conditions. After Western transfer, the blot was probed with Spr992. The molecular masses of the marker proteins are indicated on the *left* in kilodaltons (*kDa*).

Cleavage of MAT within CUB Domain II—All of the r-EK-treated r-matriptase variants were separated by SDS-PAGE under nonreducing conditions. After Western transfer, the blot was probed with Spr992. MAT, ΔS-MAT, and ΔSC1-MAT variants produced a signal at the 55-kDa position (Fig. 4*A*, *lanes 1–3*). In the sample of ΔSC1-MAT, extra signals were also produced at the positions corresponding to 150 kDa and more than

175 kDa (Fig. 4*A*, *lane 3*), suggesting that this r-matriptase variant forms complexes (trimers, tetramers) because of intermolecular disulfide bonding. ΔSC1C2-MAT and CDMAT variants gave signals at the 48- and 31-kDa positions, respectively (Fig. 4*A*, *lanes 4* and *5*). These results suggest that MAT, ΔS-MAT, and ΔSC1-MAT variants are cleaved within CUB domain II.

The 55-kDa protein from a sample of MAT was subjected to N-terminal sequencing. The phenylthiohydantoin amino acids resolved were: first, Asp (2.1 pmol)/Val (1.6 pmol); second, Val (1.3 pmol)/Arg (1.3 pmol)/Tyr (0.7 pmol); third, Gly (3.3 pmol)/Val (0.9 pmol)/Phe (0.6 pmol); fourth, Gly (3.8 pmol)/Lys (1.1 pmol)/Glu (1.0 pmol); and fifth, Leu (1.1 pmol)/Thr (0.7 pmol)/Ile (0.8 pmol). This led to the conclusion that MAT undergoes cleavage between Lys^{379} and Val^{380}, and between Lys^{399} and Asp^{400} located within CUB domain II to produce five fragments: $SerProTyr^{81}$–Gly^{149}, Ser^{150}–Lys^{379}, Val^{380}–Lys^{399}, Asp^{400}–Lys^{614}, and Val^{615}–Val^{855} (Fig. 4*B*). Note that fragment Val^{380}–Lys^{399} could be linked to fragment Asp^{400}–Lys^{614} via an intramolecular disulfide bond formed between Cys^{397} and Cys^{410} (Fig. 4*B*) (10, 41).

Cleavage of CUB Domain II by the MAT Variant Itself—P4-(Arg)P3-(Asn)P2-(Val)P1-(Lys) (refer to Fig. 4*B*) is one of the preferred cleavage sequences for matriptase (19). We hypothesized that the cleavage between Lys^{379} and Val^{380} occurs via intramolecular or intermolecular interactions of MAT molecules in the *in vitro* activation step. In the present study, we prepared a site-directed mutant of pro-MAT in which a Ser residue corresponding to the active site of matriptase (Ser^{805}) was replaced with an Ala residue (pro-S805A-MAT) in the CHO-K1 expression system. This mutant is expected to be impaired with respect to the activity of matriptase. Unless r-EK-treated pro-S805A-MAT (hereinafter S805A-MAT) underwent cleavage within CUB domain II, a self-catalyzed mechanism for the cleavage in the MAT variant would be indicated.

Samples of pro-S805A-MAT and S805A-MAT produced dense signals at the 90- and 30-kDa positions, respectively, upon reducing SDS-PAGE and Western blotting with Spr992 (Fig. 4*C*). These results indicate that pro-S805A-MAT was cleaved by r-EK at the N-terminal peptide bond of the residue corresponding to matriptase Val^{615}. S805A-MAT exhibited no detectable activity toward Sp-tPA and Boc-D(Obzl)PR-MCA, confirming the loss of matriptase activity in this mutant. Under nonreducing SDS-PAGE conditions, pro-S805A-MAT and S805A-MAT gave signals at the 83- and 84-kDa positions, respectively (Fig. 4*C*). The production of a dense signal at the 84-kDa position indicates that S805A-MAT did not undergo cleavage within CUB domain II. In addition, reducing SDS-PAGE and silver staining of S805A-MAT detected a protein band at the 64-kDa position that may correspond to matriptase Ser^{150} to Arg^{614} part, whereas those of MAT did not (supplemental Fig. S1). We conclude that the 55-kDa form of MAT (Fig. 4*A*, *lane 1*) is a result of the r-matriptase self-catalytic cleavage.

Inhibition by HAI-1–58K of MAT Purified by Benzamidine Sepharose Chromatography—To remove the fragment $SerProTyr^{81}$–Lys^{379} (hereinafter called fragment Tyr^{81}–Lys^{379}, Fig. 4*B*), MAT was treated with an immobilized benzamidine.

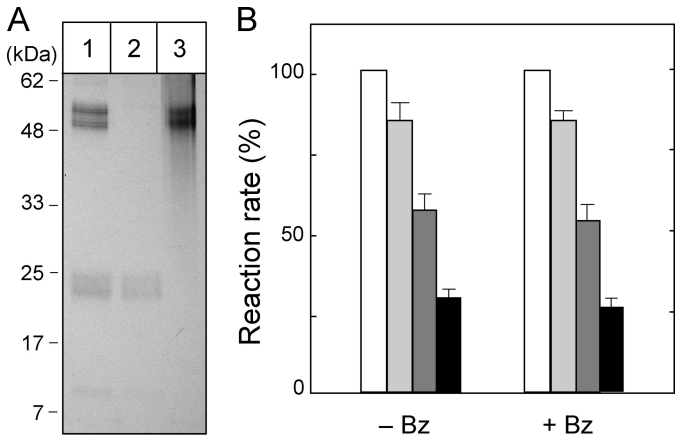

FIGURE 5. **Inhibition by HAI-1–58K of MAT molecules with and without purification by benzamidine chromatography.** *A*, SDS-PAGE and silver staining showing the removal of fragment Tyr^{81}–Lys^{379}. MAT before treatment with immobilized benzamidine (*lane 1*), the flow-through fraction of the benzamidine-precipitation procedure (*lane 2*), and the benzamidine precipitants (*lane 3*) were subjected to SDS-PAGE (12% polyacrylamide) under nonreducing conditions followed by silver staining. The positions at which the marker proteins migrated are indicated on the *left* in kilodaltons (*kDa*). *B*, inhibition of MAT without (−*Bz*) and with (+*Bz*) the benzamidine-precipitation procedure. Reactions were initiated by adding the MAT preparations at a final concentration of 1 nM to a mixture containing 1.1 mM Boc-D(Obzl)PR-MCA and HAI-1–58K. The concentrations of HAI-1–58K were 0 nM (*white*), 5 nM (*light gray*), 10 nM (*dark gray*), and 20 nM (*black*). The initial rate of hydrolysis in the absence of inhibitor was about 4 nM s^{-1} and was taken as 100% in each preparation. All values are expressed as means ± S.D. of triplicate determination.

MAT before treatment with benzamidine, the precipitants on the benzamidine resin, and the flow-through fraction of benzamidine-precipitation procedure were analyzed by SDS-PAGE under nonreducing conditions and silver staining. A sample of MAT before treatment with benzamidine produced protein bands at the 55-, 50-, 24-, 22-, and 10-kDa positions (Fig. 5*A*, *lane 1*). The flow-through fraction of the benzamidine-precipitation procedure gave 24-, 22-, and 10-kDa bands (Fig. 5*A*, *lane 2*). The sample of the precipitants with benzamidine produced signals at the 55- and 50-kDa positions (Fig. 5*A*, *lane 3*). These results indicate that the MAT after treatment with benzamidine resin is free of fragment Tyr^{81}–Lys^{379}. Judging from the sizes, the 24/22- and 10-kDa bands are thought to correspond to fragment Ser^{150}–Lys^{379} and Tyr^{81}–Gly^{149}, respectively (refer to Fig. 4*B*). The 50-kDa protein may represent fragment Val^{380}–Val^{855}, which is not cleaved between Lys^{399} and Asp^{400}. Alternatively, it may be produced via cleavage within residues Asp^{400} to Pro^{452}. In the hydrolysis of Boc-D(Obzl)PR-MCA, the MAT preparations with and without benzamidine treatment were inhibited by HAI-1–58K with similar efficiency (Fig. 5*B*). This suggests that the effect of CUB domain II on the inhibition of MAT by HAI-1–58K is mediated by residues Val^{380} to Pro^{452} but not by residues Cys^{340} to Lys^{379}.

Inhibition of CDMAT with r-HAI Variants in the Presence of C2 Peptides—We synthesized four peptides (C2 peptides) comprising 10 amino acid residues: C2P1, corresponding to Ile^{370}–Lys^{379}; C2P2, corresponding to Asn^{375}–Leu^{384}; C2P3, corresponding to Val^{380}–Asp^{389}; and C2P4, corresponding to Phe^{382}–Asn^{391} (Fig. 6*A*). We investigated their effects on the inhibition of CDMAT by HAI-1–58K using Boc-D(Obzl)PR-MCA as a substrate. The inclusion of C2P3 increased the inhi-

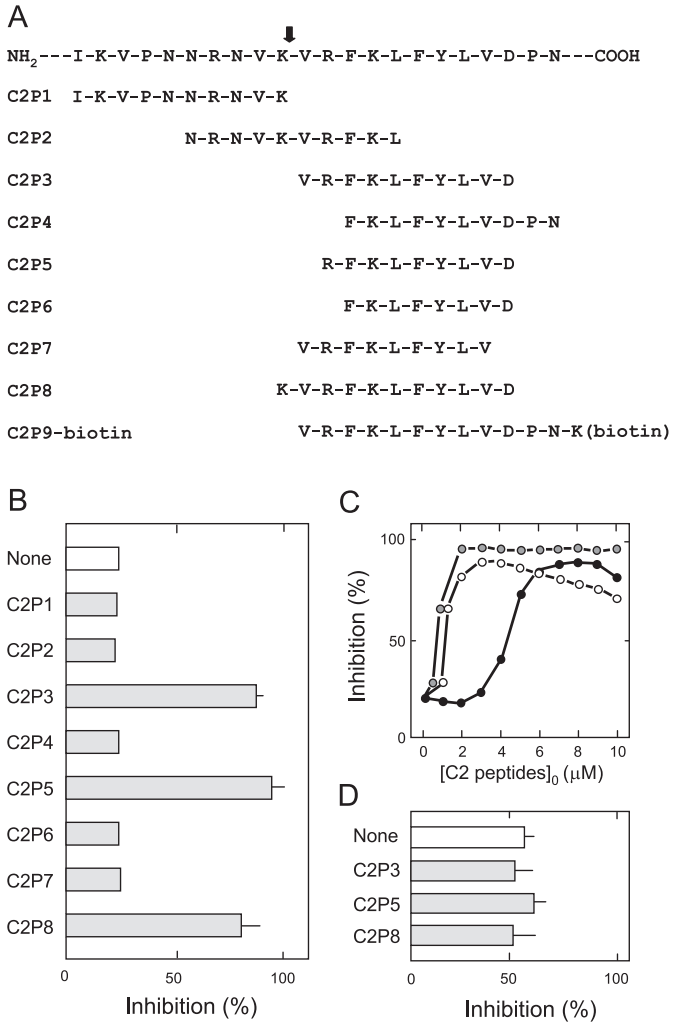

FIGURE 6. **Inhibition of CDMAT by HAI-1–58K and HAI-1–40K in the presence of C2 peptides.** *A*, sequences of C2 peptides. The sequence of Ile^{369} to Asn^{392} of rat matriptase is shown on the *top*. The cleavage site between Lys^{379} and Val^{380} is indicated by the *arrow*. The sequences of each peptide (C2P1, C2P2, C2P3, C2P4, C2P5, C2P6, C2P7, C2P8, and C2P9-biotin) are indicated. *B*, effects of C2P1 to C2P8 peptides on the inhibition of CDMAT by HAI-1–58K. The reactions were initiated by adding CDMAT at a final concentration of 1 nM to a mixture containing 5.5 nM HAI-1–58K, 1.1 mM Boc-D(Obzl)PR-MCA, and 11 μM C2 peptides. *C*, dose-dependent effects of C2P3 (*black circles*), C2P5 (*gray circles*), and C2P8 (*white circles*) on the inhibition of CDMAT by HAI-1–58K. The reaction was initiated by adding CDMAT at a final concentration of 1 nM to a mixture containing 5.5 nM HAI-1–58K, 1.1 mM Boc-D(Obzl)PR-MCA, and C2 peptides (concentrations indicated). The *y* axis shows the percentage of inhibition. *D*, inhibition of CDMAT by HAI-1–40K in the presence of C2P3, C2P5, or C2P8. The reaction was initiated by adding CDMAT at a final concentration of 1 nM to a mixture containing 1.3 nM HAI-1–40K, 1.1 mM Boc-D(Obzl)PR-MCA, and 11 μM C2 peptides. In *B* and *D*, the *x* axis shows the percentage of inhibition, and the values are expressed as means ± S.D. of triplicate determinations. *None* indicates the inhibition of CDMAT by HAI-1–58K and HAI-1–40K in the absence of C2 peptides.

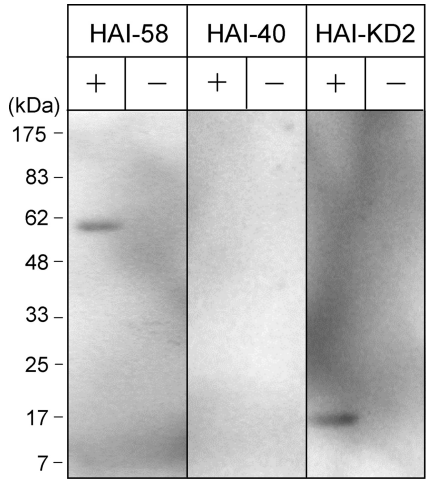

FIGURE 7. **Binding of r-HAI-1 variants to immobilized C2P9-biotin.** HAI-1–58K (HAI-58), HAI-1–40K (HAI-40), and HAI-KD2 were incubated with immobilized streptavidin resins alone (−) and with the resin to which C2P9-biotin was bound (+). After incubation, the resin was washed with HEPES buffer and boiled in the presence of Laemmli buffer. Eluates were analyzed by SDS-PAGE (12% polyacrylamide) under reducing conditions and Western blotting with horseradish peroxidase-conjugated S-protein. The positions at which the marker proteins migrate are indicated on the *left* in kilodaltons (*kDa*).

bition of CDMAT by HAI-1–58K, whereas inclusion of C2P1, C2P2, and C2P4 did not in the concentration range of 0.1 to 10 μM (Fig. 6*B*). The effect of C2P3 was sigmoidal, with maximal activity at around 8 μM (Fig. 6*C*). To identify the amino acid residues of C2P3 essential for this effect, an additional three C2 peptides (C2P5 (Arg^{381}–Asp^{390}), C2P6 (Phe^{382}–Asp^{390}), and C2P7 (Val^{380}–Val^{389})) were synthesized (Fig. 6*A*). The addition of C2P5 increased the inhibition of CDMAT by HAI-1–58K (Fig. 6*B*). The effect of C2P5 reached plateau levels at around 2 μM (Fig. 6*C*). C2P6 and C2P7 exhibited no effects in the concentration range of 0.1 to 10 μM (Fig. 6*B*), indicating that residues Arg^{381} to Asp^{390} are indispensable for the effect. The ability of C2P5 to increase the CDMAT-inhibiting activity of HAI-1–58K suggests that the α-amino group of Val^{380} is not involved in the effect of C2P3. To validate this conclusion, the effect of C2P8 (Lys^{379}–Asp^{390}; Fig. 6*A*) was examined further. C2P8 increased the inhibition of CDMAT by HAI-1–58K (Fig. 6*B*), with maximal effect at around 3 μM (Fig. 6*C*). None of the C2 peptides significantly increases the inhibition of CDMAT by HAI-1–40K. For instance, the degree of inhibition of CDMAT by 1.2 nM HAI-1–40K in the absence of C2 peptide was similar to that in the presence of 10 μM C2P3, C2P5, or C2P8 (Fig. 6*D*).

Binding of r-HAI-1 Variants to C2P9-biotin—Results shown in Fig. 6*B* led to the hypothesis that residues Arg^{381} to Asp^{390} in CUB domain II bind to HAI-1–58K and cause a conformational change in the r-HAI-1 variant that increases the matriptase-inhibiting activity. For this reason, we examined whether CUB domain II residues (Arg^{381} to Asp^{390}) interact directly with HAI-1–58K. C2P9-biotin is a synthetic peptide comprising residues Val^{380} to Pro^{392} with a C-terminal lysine residue in which the ϵ-amino group is biotinylated (Fig. 6*A*). HAI-1–58K (indicated by a 59-kDa band in SDS-PAGE) (28) was precipitated with immobilized streptavidin resins to which C2P9-biotin bound but not with immobilized streptavidin resins alone (Fig. 7). By contrast, HAI-1–40K (indicated by a 41-kDa band in SDS-PAGE) (28) did not appear to bind to immobilized C2P9-biotin (Fig. 7, HAI-1–40K, *lane* +). This is consistent with the observation that C2 peptides such as C2P3 did not increase the matriptase-inhibiting activity of HAI-1–40K (Fig. 6*D*). This also suggests that CUB domain II (Arg^{381} to Asp^{390}) interacts with the LDLRA domain or Kunitz domain II of HAI-1–58K.

HAI-KD2 is a secreted variant of r-HAI-1 comprising only Kunitz domain II. This r-HAI-1 variant inhibits bovine trypsin but not MAT (28). HAI-KD2 (indicated by a 17-kDa band in

SDS-PAGE) (28) was precipitated with immobilized streptavidin resins to which C2P9-biotin bound but not with immobilized streptavidin resins alone (Fig. 7).

DISCUSSION

The results of the present study indicate that CUB domain II is responsible for facilitating the primary inhibitory interaction with HAI-1–58K. This CUB domain is a widely occurring module in proteolytic enzymes or proteins that are involved in developmental processes such as urchin embryonic growth factor (41, 42). The domain comprises about 110 amino acid residues and has conserved characteristics, which include the presence of four cysteine residues (*i.e.* two disulfide bonds) and various conserved hydrophobic and aromatic positions (41). Crystallographic studies show that CUB domains comprise 10 β-strands that are organized into two five-stranded β-sheets (43–45). Importantly, the CUB domains in certain proteases are essential for recognition of natural substrates; *e.g.* the interactions between complement proteases C1r and C1s (46), between the second CUB domain of bone morphogenetic protein-1 and procollagen C (47, 48), and between the first CUB domain of ADAMTS13 (a disintegrin and metalloprotease with a thrombospondin motif) and von Willebrand factor (49). However, there is no evidence that the CUB domains of matriptase play essential roles in the recognition of substrates, including sc-uPA, pro-HGF, and prostasin precursor (18–21, 29, 40). A bacterially expressed chimera protein comprising glutathione *S*-transferase and the two CUB domains of matriptase was found previously to bind to a transmembrane protein with epidermal growth factor-like and two follistatin-like 1 domains (50). However, it is unclear whether the transmembrane protein serves as a substrate for matriptase. Regardless, the present findings provide the first evidence that the CUB domain in a proteolytic enzyme might serve to down-regulate its own catalytic activity.

HAI-1–40K inhibits MAT with greater efficiency than does HAI-1–58K (28). Similar results were observed for the inhibition of a pro-HGF-converting enzyme (HGF activator) (32, 51). In addition, in the context of the 58-kDa HAI-1, the HGF activator binding of each Kunitz domain is affected by the presence of other Kunitz domain, suggesting that the two protease-binding sites in the HAI-1 species are close to each other (52). In other words, the protease-inhibiting site of Kunitz domain I is thought to be obstructed by that of Kunitz domain II in the context of HAI-1–58K (Fig. 8, *left*). In the present study, we found that (i) C2P5 increased the inhibition of CDMAT by HAI-1–58K but not that by HAI-1–40K and that (ii) HAI-1–58K and HAI-KD2 precipitated with resins to which C2P9-biotin was bound. Considering these findings, we propose that residues Arg^{381} to Asp^{390} in CUB domain II binds to Kunitz domain II in the context of HAI-1–58K and that this binding causes a conformational change of the r-HAI-1 variant in a way that prevents the obstruction of Kunitz domain I (Fig. 8, *right*). This could be the reason why MAT is more strongly inhibited by HAI-1–58K than is CDMAT. At present, however, the molecular mechanisms for the interaction between C2P9-biotin and HAI-KD2 are unclear. Experiments with additional sets of C2 peptides and HAI-KD2 mutants would allow us to explore these mechanisms.

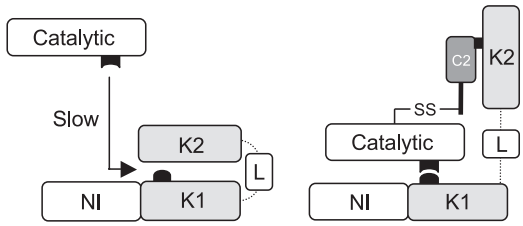

FIGURE 8. **A schematic model of the interaction of CDMAT and MAT with HAI-1–58K.** The putative domain organization of HAI-1–58K is shown on the *left*. CDMAT is also indicated. The spacer region of HAI-1–58K is indicated by the *dashed curve*. The interaction between MAT where the Tyr^{81}–Lys^{379} fragment is absent and HAI-1–58K is illustrated on the *right*. The disulfide bond formed between the stem and catalytic domains of MAT is indicated by *SS*. In each illustration, the protease-inhibiting site of Kunitz domain I is indicated by a *black semicircle*. The site of interaction with Kunitz domain I in MAT and CDMAT variants is indicated by the *semicircle in the rectangle* (*black*). The residues Arg^{381} to Asp^{390} in CUB domain II (C2) are indicated by the *solid square*. The N-terminal and internal domains of HAI-1–58K are illustrated as *one rectangle* (*NI*). *Catalytic*, catalytic domain of matriptase; *K1*, Kunitz domain I; *K2*, Kunitz domain II; *L*, LDLRA domain of HAI-1–58K.

In the present study, we provided evidence that the cleavage between Lys^{379} and Val^{380} located within CUB domain II in the MAT variant occurs via intramolecular or intermolecular interactions of the molecules in the *in vitro* activation step. ΔS- and ΔSC1-MAT variants may be cleaved at the same site by a similar mechanism. It is, however, unclear whether, in the context of MAT, the cleavage is essential for interaction of CUB domain II (Arg^{381}–Asp^{390}) with HAI-1–58K. The HAI-1–58K-activating activity of C2P8 does not support the requirement of the cleavage. Matriptase purified from human milk has been found to produce protein bands at the 70- and 50-kDa positions in SDS-PAGE under nonreducing conditions (53). N-terminal sequencing analysis showed that the 70-kDa protein is a disulfide-linked two-chain active form of this protease comprising CUB domain I to the catalytic domain (53). Judging from the size, the 50-kDa band might be another active form with an N terminus within CUB domain II (possibly at Val^{380}). Therefore, we cannot exclude the possibility that the cleavage after Lys^{379} in the context of native matriptase facilitates the interaction of CUB domain II (Arg^{381}-Asp^{390}) with the 58-kDa HAI-1 species.

In summary, we have provided evidence that matriptase CUB domain II serves as the secondary site for interaction with HAI-1 with the entire extracellular domain and facilitates the primary inhibitory interaction. The catalytic activity of matriptase must be tightly regulated *in vivo* because prolonged activity is harmful to cells (1). The occurrence of the 40-kDa HAI-1 species is probably a mechanism for the rapid and efficient down-regulation of matriptase activity (28). The interaction of CUB domain II with HAI-1 (with Kunitz domain II) might also be one important mechanism for preventing the prolonged activity of matriptase.

Acknowledgments—We thank Yuka Miyake and Yukari Matsuno for helpful discussions and assistance during this investigation.

REFERENCES

1. Lin, C. Y., Tseng, I. C., Chou, F. P., Su, S. F., Chen, Y. W., Johnson, M. D., and Dickson, R. B. (2008) *Front. Biosci.* **13,** 621–635

2. Darragh, M. R., Bhatt, A. S., and Craik, C. S. (2008) *Front. Biosci.* **13,** 528–539
3. Bugge, T. H., List, K., and Szabo, R. (2007) *Front. Biosci.* **12,** 5060–5070
4. Kim, M. G., Chen, C., Lyu, M. S., Cho, E. G., Park, D., Kozak, C., and Schwartz, R. H. (1999) *Immunogenetics* **49,** 420–428
5. Zhang, Y., Cai, X., Schlegelberger, B., and Zheng, S. (1998) *Cytogenet. Cell Genet.* **83,** 56–57
6. Zeng, L., Cao, J., and Zhang, X. (2005) *World J. Gastroenterol.* **11,** 6202–6207
7. Satomi, S., Yamasaki, Y., Tsuzuki, S., Hitomi, Y., Iwanaga, T., and Fushiki, T. (2001) *Biochem. Biophys. Res. Commun.* **287,** 995–1002
8. Szabo, R., and Bugge, T. H. (2008) *Int. J. Biochem. Cell Biol.* **40,** 1297–1316
9. Qiu, D., Owen, K., Gray, K., Bass, R., and Ellis, V. (2007) *Biochem. Soc. Trans.* **35,** 582–1587
10. Takeuchi, T., Shuman, M. A., and Craik, C. S. (1999) *Proc. Natl. Acad. Sci. U.S.A.* **96,** 11054–11061
11. Cho, E. G., Kim, M. G., Kim, C., Kim, S. R., Seong, I. S., Chung, C., Schwartz, R. H., and Park, D. (2001) *J. Biol. Chem.* **276,** 44581–44589
12. Oberst, M. D., Williams, C. A., Dickson, R. B., Johnson, M. D., and Lin, C. Y. (2003) *J. Biol. Chem.* **278,** 26773–26779
13. Oberst, M. D., Chen, L. Y., Kiyomiya, K., Williams, C. A., Lee, M. S., Johnson, M. D., Dickson, R. B., and Lin, C. Y. (2005) *Am. J. Physiol. Cell Physiol.* **289,** C462–C470
14. Miyake, Y., Yasumoto, M., Tsuzuki, S., Fushiki, T., and Inouye, K. (2009) *J. Biochem.* **146,** 273–282
15. Miyake, Y., Tsuzuki, S., Mochida, S., Fushiki, T., and Inouye, K. (2010) *Biochim. Biophys. Acta* **1804,** 156–165
16. Inouye, K., Yasumoto, M., Tsuzuki, S., Mochida, S., and Fushiki, T. (2010) *J. Biochem.* **147,** 485–492
17. Wang, J. K., Lee, M. S., Tseng, I. C., Chou, F. P., Chen, Y. W., Fulton, A., Lee, H. S., Chen, C. J., Johnson, M. D., and Lin, C. Y. (2009) *Am. J. Physiol. Cell Physiol.* **297,** C459–C470
18. Lee, S. L., Dickson, R. B., and Lin, C. Y. (2000) *J. Biol. Chem.* **275,** 36720–36725
19. Takeuchi, T., Harris, J. L., Huang, W., Yan, K. W., Coughlin, S. R., and Craik, C. S. (2000) *J. Biol. Chem.* **275,** 26333–26342
20. Kirchhofer, D., Peek, M., Li, W., Stamos, J., Eigenbrot, C., Kadkhodayan, S., Elliott, J. M., Corpuz, R. T., Lazarus, R. A., and Moran, P. (2003) *J. Biol. Chem.* **278,** 36341–36349
21. Netzel-Arnett, S., Currie, B. M., Szabo, R., Lin, C. Y., Chen, L. M., Chai, K. X., Antalis, T. M., Bugge, T. H., and List, K. (2006) *J. Biol. Chem.* **281,** 32941–32945
22. Oberst, M. D., Singh, B., Ozdemirli, M., Dickson, R. B., Johnson, M. D., and Lin, C. Y. (2003) *J. Histochem. Cytochem.* **51,** 1017–1025
23. List, K., Hobson, J. P., Molinolo, A., and Bugge, T. H. (2007) *J. Cell. Physiol.* **213,** 237–245
24. List, K., Haudenschild, C. C., Szabo, R., Chen, W., Wahl, S. M., Swaim, W., Engelholm, L. H., Behrendt, N., and Bugge, T. H. (2002) *Oncogene* **21,** 3765–3779
25. List, K., Szabo, R., Wertz, P. W., Segre, J., Haudenschild, C. C., Kim, S. Y., and Bugge, T. H. (2003) *J. Cell Biol.* **163,** 901–910
26. Szabo, R., Kosa, P., List, K., and Bugge, T. H. (2009) *Am. J. Pathol.* **174,** 2015–2022
27. List, K., Kosa, P., Szabo, R., Bey, A. L., Wang, C. B., Molinolo, A., and Bugge, T. H. (2009) *Am. J. Pathol.* **175,** 1453–1463
28. Kojima, K., Tsuzuki, S., Fushiki, T., and Inouye, K. (2008) *J. Biol. Chem.* **283,** 2478–2487
29. Kojima, K., Tsuzuki, S., Fushiki, T., and Inouye, K. (2009) *Biosci. Biotechnol. Biochem.* **73,** 454–456
30. Shimomura, T., Denda, K., Kitamura, A., Kawaguchi, T., Kito, M., Kondo, J., Kagaya, S., Qin, L., Takata, H., Miyazawa, K., and Kitamura, N. (1997) *J. Biol. Chem.* **272,** 6370–6376
31. Szabo, R., Molinolo, A., List, K., and Bugge, T. H. (2007) *Oncogene* **26,** 1546–1556
32. Shimomura, T., Denda, K., Kawaguchi, T., Matsumoto, K., Miyazawa, K., and Kitamura, N. (1999) *J. Biochem.* **126,** 821–828
33. Tsuzuki, S., Murai, N., Miyake, Y., Inouye, K., Hirayasu, H., Iwanaga, T., and Fushiki, T. (2005) *Biochem. J.* **388,** 679–687
34. Miyake, Y., Tsuzuki, S., Yasumoto, M., Fushiki, T., and Inouye, K. (2009) *Cytotechnology* **60,** 95–103
35. Kojima, K., Tsuzuki, S., Fushiki, T., and Inouye, K. (2009) *J. Biochem.* **145,** 783–790
36. Yamasaki, Y., Satomi, S., Murai, N., Tsuzuki, S., and Fushiki, T. (2003) *J. Nutr. Sci. Vitaminol.* **49,** 27–32
37. Laemmli, U. K. (1970) *Nature* **227,** 680–685
38. Tsuzuki, S., Kokado, Y., Satomi, S., Yamasaki, Y., Hirayasu, H., Iwanaga, T., and Fushiki, T. (2003) *Biochem. J.* **372,** 227–233
39. Murai, N., Miyake, Y., Tsuzuki, S., Inouye, K., and Fushiki, T. (2009) *Cytotechnology* **59,** 169–176
40. Mochida, S., Tsuzuki, S., Yasumoto, M., Inouye, K., and Fushiki, T. (2009) *Enzyme Microb. Technol.* **45,** 288–294
41. Bork, P., and Beckmann, G. (1993) *J. Mol. Biol.* **231,** 539–545
42. Hursh, D. A., Andrews, M. E., and Raff, R. A. (1987) *Science* **237,** 1487–1490
43. Gregory, L. A., Thielens, N. M., Arlaud, G. J., Fontecilla-Camps, J. C., and Gaboriaud, C. (2003) *J. Biol. Chem.* **27,** 32157–32164
44. Varela, P. F., Romero, A., Sanz, L., Romão, M. J., Töpfer-Petersen, E., and Calvete, J. J. (1997) *J. Mol. Biol.* **274,** 635–649
45. Feinberg, H., Uitdehaag, J. C., Davies, J. M., Wallis, R., Drickamer, K., and Weis, W. I. (2003) *EMBO J.* **22,** 2348–2359
46. Thielens, N. M., Enrie, K., Lacroix, M., Jaquinod, M., Hernandez, J. F., Esser, A. F., and Arlaud, G. J. (1999) *J. Biol. Chem.* **274,** 9149–9159
47. Hulmes, D. J., Mould, A. P., and Kessler, E. (1997) *Matrix Biol.* **16,** 41–45
48. Hartigan, N., Garrigue-Antar, L., and Kadler, K. E. (2003) *J. Biol. Chem.* **278,** 18045–18049
49. Tao, Z., Peng, Y., Nolasco, L., Cal, S., Lopez-Otin, C., Li, R., Moake, J. L., López, J. A., and Dong, J. F. (2005) *Blood* **106,** 4139–4145
50. Ge, W., Hu, H., Ding, K., Sun, L., and Zheng, S. (2006) *J. Biol. Chem.* **281,** 7406–7412
51. Miyazawa, K., Shimomura, T., Kitamura, A., Kondo, J., Morimoto, Y., and Kitamura, N. (1993) *J. Biol. Chem.* **268,** 10024–10028
52. Denda, K., Shimomura, T., Kawaguchi, T., Miyazawa, K., and Kitamura, N. (2002) *J. Biol. Chem.* **277,** 14053–14509
53. Benaud, C., Dickson, R. B., and Lin, C. Y. (2001) *Eur. J. Biochem.* **268,** 1439–1447